Efficient Role of Optical Fiber Modulators for High Speed Optical Communications Systems Applications

Mohamed A. Metawe'e
Higher Institute of Engineering and Technology in El-Arish, EGYPT

***Abstract*— Optical components and integrated optical devices that operate at high frequency and with high bandwidth are necessary for next generation high transmission capacity network applications. This paper has proposed the high reliability and efficient role of optical fiber electro-optic modulator devices in high speed optical communications systems applications. We have taken into account the study of cut-off frequency, 3-dB bandwidth, modulation bandwidth, transmission bit rates and products within non return to zero coding over wide range of the controlling parameters.**

***Index Terms*— Modulation bandwidth, Switching voltage, 3-dB bandwidth, Cut-off frequency, and Transmission capacity.**

I. INTRODUCTION

Modulators modify light signals such that they can be used to send data along optical transmission lines. The optical signal is actually modulated by an electrical signal through the use of the $LiNbO_3$ crystal [1, 2]. The crystal's indices of refraction depend proportionally on the strength of the electrical field being passed across the crystal. Thus, the extent to which the crystal modulates the phase of the light depends on the electrical signal. Basically, this means that any electrical signal, for any application, can be transformed into an optical signal simply by running the signal across the $LiNbO_3$ crystal [3, 4]. Even though, the electrical field does modulate the phase of the light propagating through the crystal, a process is necessary to provide intensity based modulation from the phase based modulation. To do this, the light signal is separated into two waveguides inside the crystal. After modulation, whether conducted on one waveguide or both the end result by joining them at the output is an intensity based modulation due to the interference of the two paths of light [5]. The optimum situation would suggest that no optical power be present for a digital "0," and that the maximum optical power be present for a digital "1." This would require either complete constructive interference, or complete destructive interference. Ideally, constructive interference occurs when the light is modulated by p radians and destructive interference occur s when the light is not modulated at all. Therefore, it is desirable to put the crystal in a state that modulates the phase so that a "1" would require Vp + p/2 and a "0" would require Vp – p/2 (directly in between the two extremes). This state is called quadrature, sometimes called Vp and it results in the best extinction ratio because complete negative voltage causes destructive interference and complete positive voltage causes constructive interference [6, 7].

In the present study, we have achieved modulation by inducing a change in the phase or the intensity of the light, using a refractive index change or an absorption change, respectively. Moreover we have analyzed parametrically the transmission data rate, operating signal bandwidth, modulation bandwidth, device performance index, and transmission data rate length product within non return to zero (NRZ) coding as a good criteria for high speed electrooptic device performance and transmission efficiency.

II. DEVICE MODELING ANALYSIS

To use the highest electrooptic coefficient in $LiNbO_3$ (r_{33}), the externally applied electric field should be parallel to the Z-axis [7]. Therefore, in order to optimize the interaction between the electric field and the optical mode [8], in a Z-cut wafer the electrodes should be positioned on top of the waveguide arms, while in an X-cut wafer the electrodes should be located on both sides of the branches. In these conditions the extraordinary refractive index change by electro-optic effect in $LiNbO_3$ is given by [9]:

$$\Delta n_e = 0.5\, n_e\, r_{33}\, E_z \ , \qquad (1)$$

Where n_e is the effective refractive index of the material based electrooptic modulator device, r_{33} is the corresponding electrooptic coefficient in pm/Volt, E_z is the applied electic field in Z-direction in Volt/cm. The integrated Mach-Zehnder intensity modulator is perhaps the paradigm of integrated optical devices, and it has been successfully used in optics communications technology. The theoretical value for the half-wave voltage of the integrated electro-optic modulator or switching voltage can be calculated using the expression [10]:

$$V_\pi = \frac{\lambda g}{L_m n_e^3 r_{33} \Gamma} \ , \qquad (2)$$

Where λ is the operating signal wavelength in μm, g is the gap between electrodes in μm, L_m is the modulator length in cm, and Γ is confinement factor (factor with relates the overlap between the applied electric field and the propagating modal field). The transmittance of an optical signal through the modulator using the following equation:

$$T_m = e^{-\alpha L_m} \ , \text{dB} \qquad (3)$$

Where α is the power absorption coefficient in dB/cm. The resistance of modulator device can be measured by estimating the device dimensions as the following equation:

$$R = \rho \frac{L_m}{wd} \ , \qquad (4)$$

Where ρ is the resistivity, d is the modulator thickness, and w is the modulator width. The time constant, τ of the modulator device can be calculated as follows [9]:

$$\tau = RC \ , \qquad (5)$$

The cut-off frequency, $f_{cut\text{-}off}$ of the modulator device is calculated from the RC time constant as the following:

$$f_{cut-off} = \frac{1}{2\pi RC} , \quad (6)$$

The relative refractive index change induces an optical phase modulation of:

$$\Delta\phi = k_0 L_m \Delta n_e , \quad (7)$$

Where $k_0=2\pi/\lambda$ is the wave number. The electrical 3-dB bandwidth $f_{3\text{-dB}}$ for which modulation voltage, V_m is reduced by $(1/\sqrt{2})$ from its value can be expressed as [10]:

$$f_{3-dB} = \frac{1}{\pi R \varepsilon_{eff} C L_m} , \quad (8)$$

Where C is the capacitance in pf, ε_{eff} is the effective RF relative dielectric constant. The bandwidth is reduced by the electrooptic device loss. Under the perfect velocity matching condition [11], achievable modulation bandwidth f_m is:

$$f_m = \frac{6.84}{\alpha L_m} , \text{ GHz} \quad (9)$$

For $LiNbO_3$ material, the investigation of both the thermal and spectral variations of the effective waveguide refractive index (n_e) require empirical equation. The set of parameters required to completely characterize the temperature dependence of the refractive-index is given below, Sellmeier equation is under the form [12]:

$$n_e = \sqrt{A_1 + A_2 H + \frac{A_3 + A_4 H}{\lambda^2 - (A_5 + A_6 H)^2} + \frac{A_7 + A_8 H}{\lambda^2 - A_9^2} - A_{10}\lambda} , \quad (10)$$

Where λ is the optical signal wavelength in μm and $H = T^2 - T_0^2$, T is the ambient temperature in K, and T_0 is the room temperature (300 K). The set of parameters of equation coefficients ($LiNbO_3$) are recast and dimensionally adjusted as: A_1=5.35583, A_2=4.629x10^{-7}, A_3=0.100473, A_4=3.862x10^{-8}, A_5=0.20692, A_6=-0.89x10^{-8}, A_7=100, A_8=2.657 x10^{-5}, A_9=11.34927, and A_{10}=0.01533. Equation (10) can be simplified as the following:

$$n_e = \sqrt{A_{12} + \frac{A_{34}}{\lambda^2 - A_{56}^2} + \frac{A_{78}}{\lambda^2 - A_9^2} - A_{10}\lambda} , \quad (11)$$

Where: $A_{12}=A_1+A_2H$, $A_{34}=A_3+A_4H$, $A_{56}=A_5+A_6H$, and $A_{78}=A_7+A_8H$. Then the first and second differentiation of Eq. (11) with respect to operating signal wavelength λ which gives:

$$\frac{dn_e}{d\lambda} = \left(\frac{-\lambda}{n_e}\right).\left(\frac{A_{34}}{\left(\lambda^2 - A_{56}^2\right)^2} + \frac{A_{78}}{\left(\lambda^2 - A_9^2\right)^2} - A_{10}\right) , \quad (12)$$

$$\frac{d^2 n_e}{d\lambda^2} = \left(\frac{1}{n_e}\right).\left(\frac{A_{34}\left(2 - \left(\lambda^2 - A_{56}^2\right)\right)}{\left(\lambda^2 - A_{56}^2\right)^2} + \frac{A_{78}\left(2 - \left(\lambda^2 - A_9^2\right)\right)}{\left(\lambda^2 - A_9^2\right)^2} + A_{10}\right) , \quad (13)$$

The material dispersion based electrooptic modulator, $D_{mat.}$ which is given by the following equation [13]:

$$D_{mat} = -\left(\frac{L_m . \Delta\lambda . \lambda}{c}\right).\left(\frac{d^2 n_e}{d\lambda^2}\right) , \quad (14)$$

The modal-dispersion delay, D_{modal} for a multi mode step-index electrooptic device with length L_m, is given by:

$$D_{modal} = L_m n_e \Delta n_e / c , \quad (15)$$

Where the total dispersion coefficient [13-15], $D_t=D_{mat.}+D_{modal}$. In addition to providing sufficient power to the receiver, the system must also satisfy the bandwidth requirements imposed by the rate at which data are transmitted. A convenient method of accounting for the bandwidth is to combine the rise times of the various system components and compare the result with the rise time needed for the given data rate and pulse coding scheme. The system rise time is given in terms of the data rate for non return to zero pulse code by [16, 17]:

$$B_R(NRZ) = \frac{0.7}{D_t} , \quad (16)$$

In the same way, the device performance index (DPI) can be expressed as the following expression [18]:

$$DPI = \frac{f_m}{V_\pi} , GHz/Volt \quad (17)$$

III. PERFORMANCE ANALYSIS

We have investigated recent progress of $LiNbO_3$ based electrooptic modulator device in high speed photonic networks over wide range of the affecting operating parameters as shown in Table 1.

Table 1: List of Simulation parameters used in electro-optic modulator device [3, 6, 8, 10].

Operating parameter	Symbol	Value
Operating signal wavelength	λ	1.3 μm—1.55 μm
Spectral line width of the optical source	$\Delta\lambda$	0.1 nm
Ambient temperature	T	300 K ≤ T ≤ 320 K
Room temperature	T_0	300 K
Relative refractive-index change	Δn_e	0.05 ≤ Δn ≤ 0.09
Modulator length	L_m	5 cm ≤ L_m ≤ 10 cm
Speed of light	c	3 x10^{10} cm/sec
Modulator width	W	2 cm ≤ W ≤ 5 cm
Modulator thickness	d	0.2 cm ≤ d ≤ 1 cm
Gap between electrodes	g	0.1–0.35 μm
Electro-optic coefficient	r_{33}	30.8x10^{-10} cm/Volt
Applied electric field	E	2 Volt/cm
Resistivity	ρ	2.66x10^{-3} Ω.cm
Confinement factor	Γ	0.8–0.95
Modulator device capacitance	C	0.2–0.4 nF
Effective RF relative dielectric constant	ε_{eff}	17.85
Power absorption coefficient	α	0.1–0.4 dB/cm

Based on the model equations analysis, assumed set of the operating parameters, and the set of the Figs. (2–12), the following facts are assured as the following results:

i) Fig. 1 has assured that as the operating optical signal wavelength increases, this leads to decrease in device performance index at constant power absorption coefficient. As well as power absorption coefficient increases, this results in decreasing of device performance at constant operating optical signal wavelength.

ii) As shown in Fig. 2 has proved that as operating optical signal wavelength increases, this leads to increase in switching voltage at constant modulator length. As well as modulator length increases, this

results in decreasing of switching voltage at constant operating optical signal wavelength.

iii) Fig. 3 has demonstrated that as gap between electrodes increases, this leads to decrease in device performance index at constant confinement factor. As well as confinement factor increases, this results of increasing of device performance index at constant gap between electrodes.

iv) Fig. 4has indicated that as ambient temperature increases, this leads to slightly decreases in switching voltage at gap between electrodes. As well as gap between electrodes increases, this results of increasing of switching voltage at constant ambient temperature.

v) As shown in Fig. 5 has assured as both modulator length and power absorption coefficient increase, this results in decreasing of modulator transmittance.

vi) Fig. 6 has proved that as both modulator width and modulator thickness increase this leads to decrease of time constant of the modulator devices.

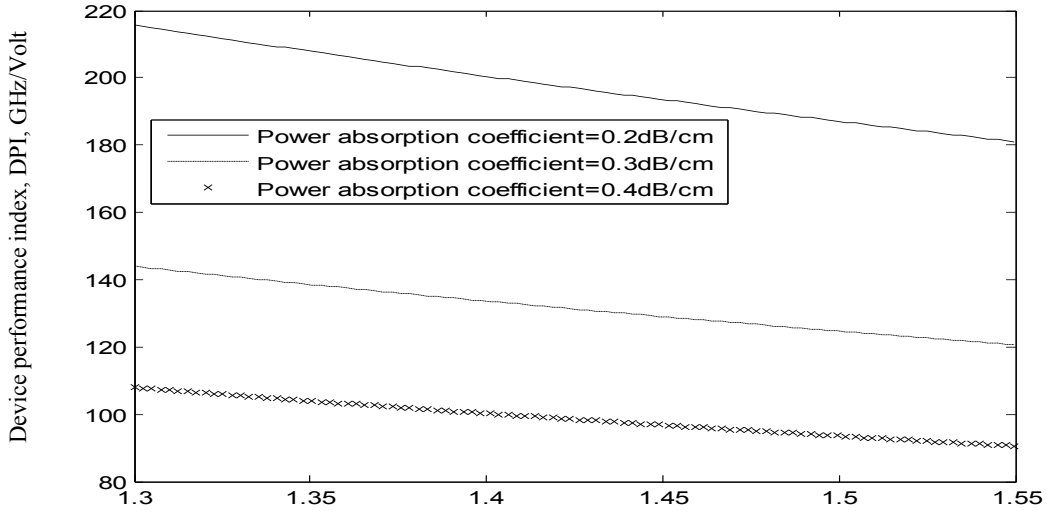

Fig. 1. Variations of the device performance index versus operating signal wavelength at the assumed set of parameters.

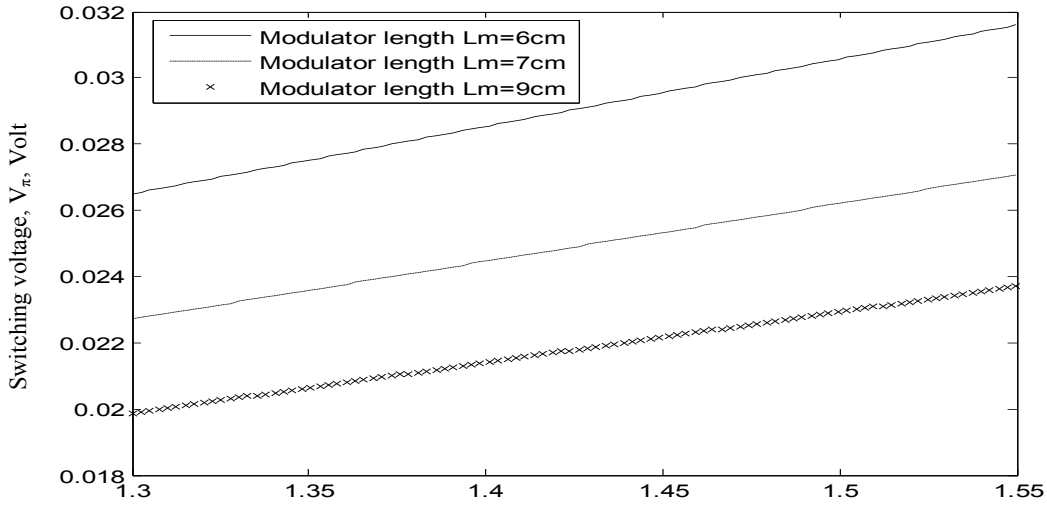

Fig. 2. Variations of the switching voltage versus operating signal wavelength at the assumed set of parameters.

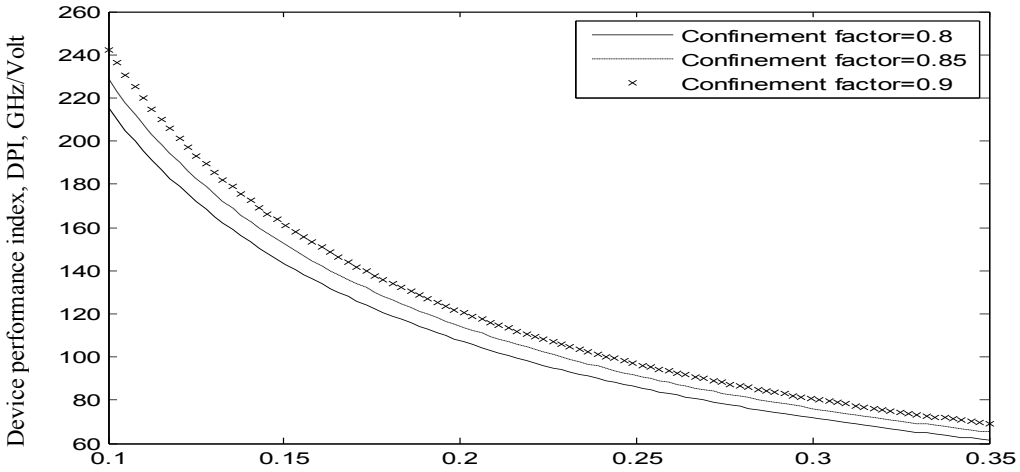

Fig. 3. Variations of the device performance index against gap between electrodes at the assumed set of parameters.

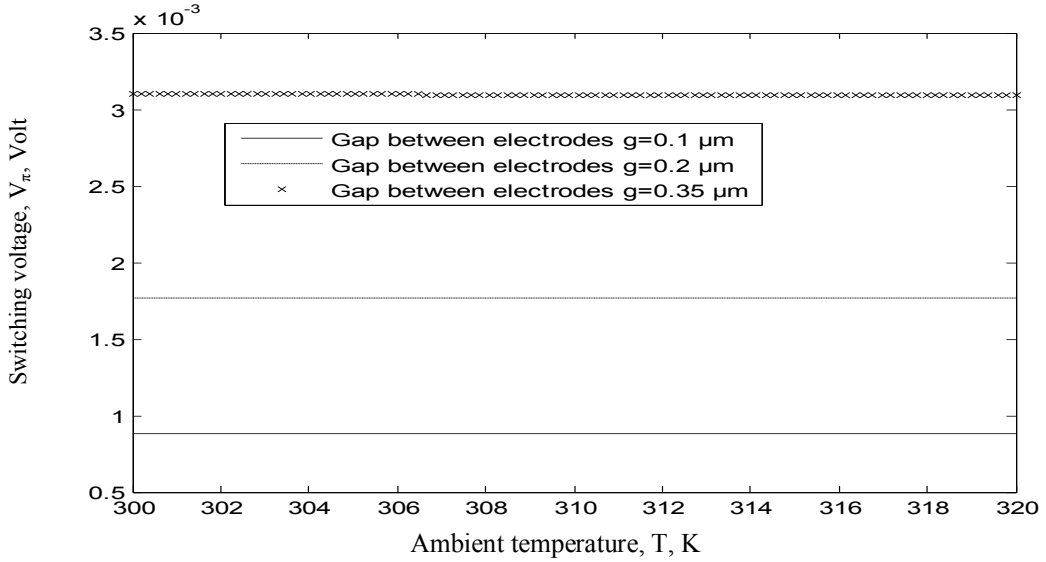

Fig. 4. Variations of the switching voltage against ambient temperature at the assumed set of parameters.

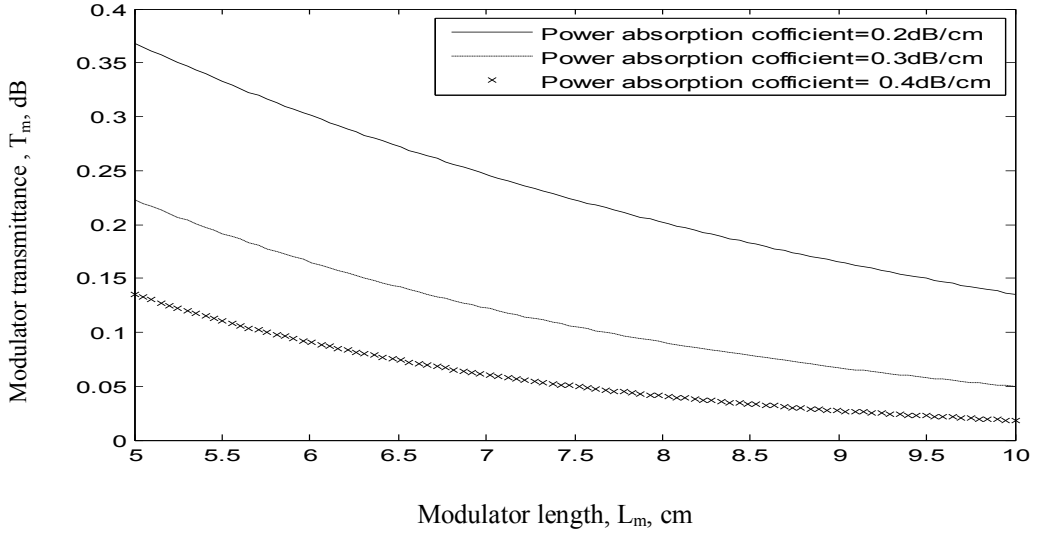

Fig. 5. Variations of the modulator transmittance against modulator length at the assumed set of parameters.

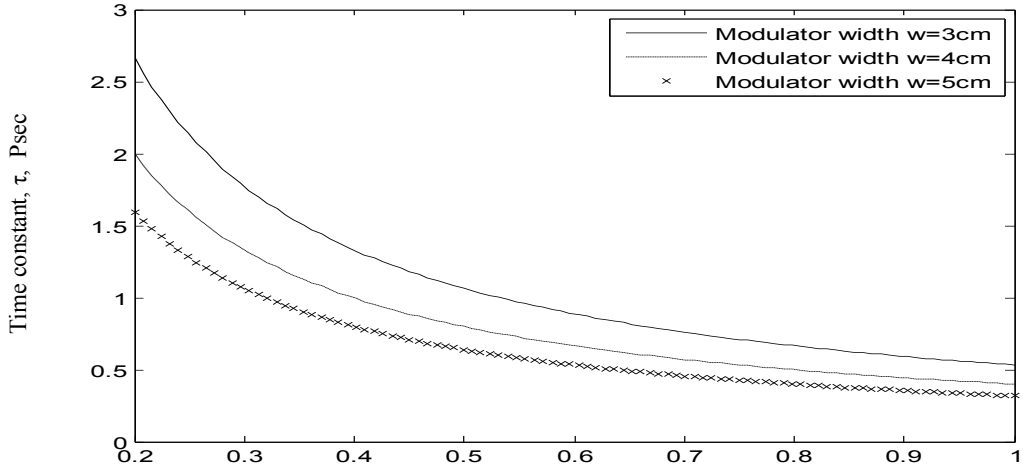

Fig. 6. Variations of modulator time constant against modulator thickness at the assumed set of parameters.

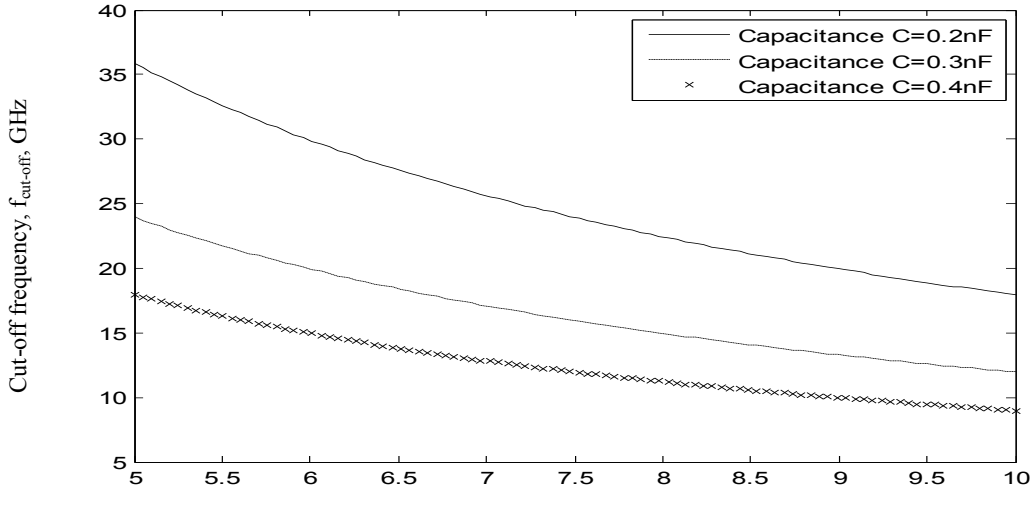

Fig. 7. Variations of cut-off frequency against modulator length at the assumed set of parameters.

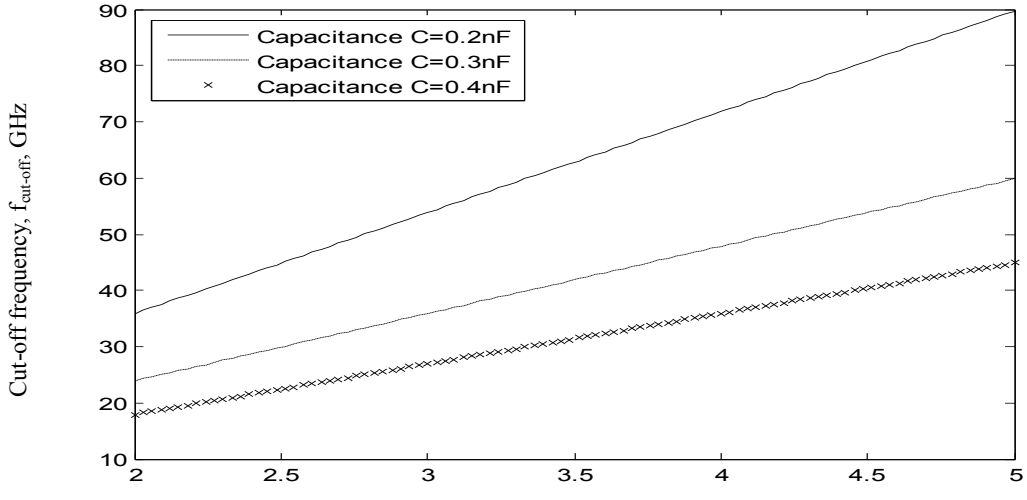

Fig. 8. Variations of cut-off frequency against modulator width at the assumed set of parameters.

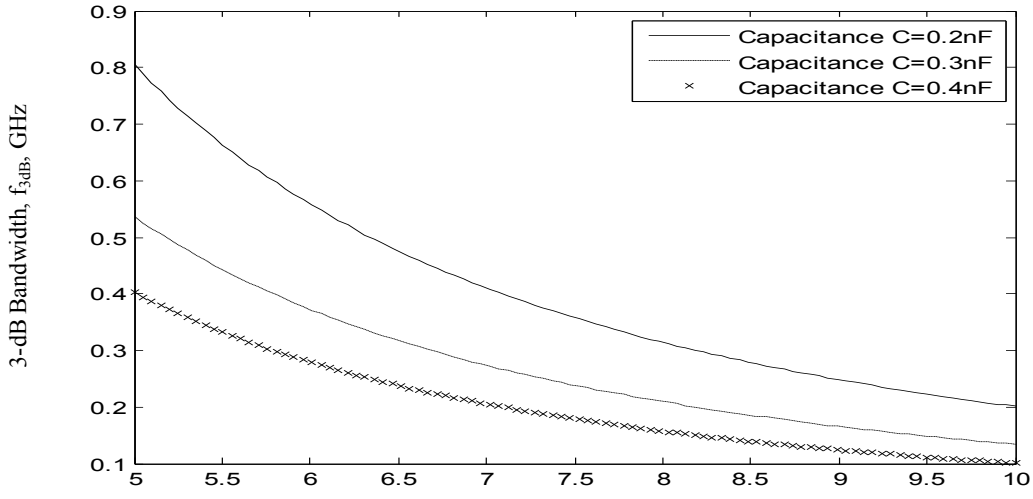

Fig. 9. Variations of 3-dB bandwidth against modulator length at the assumed set of parameters.

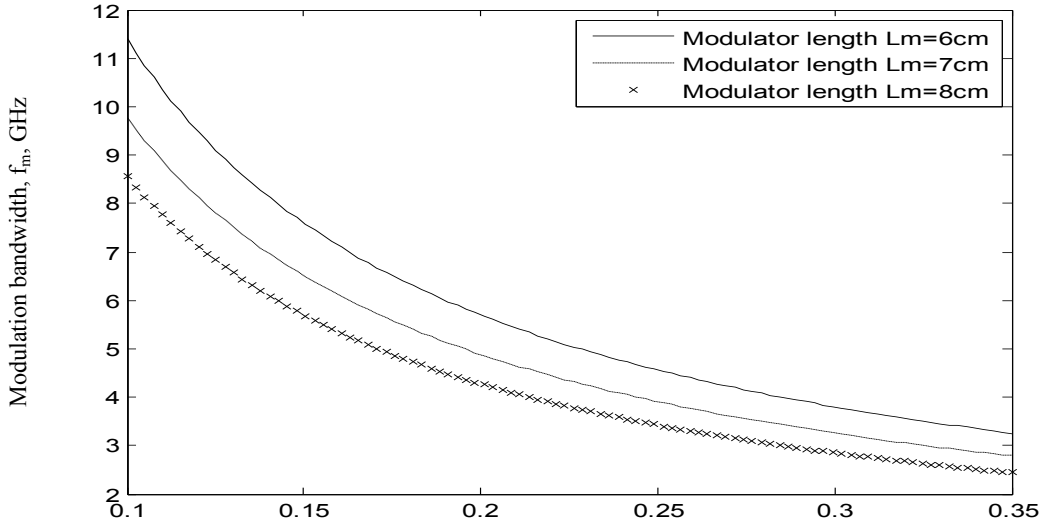

Fig. 10. Variations of modulation bandwidth against power absorption coefficient at the assumed set of parameters.

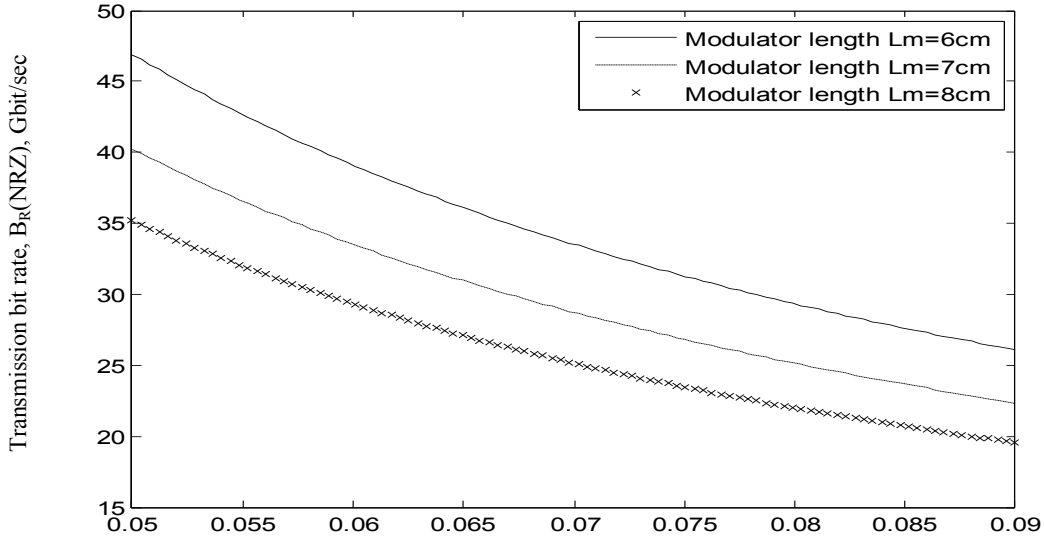

Fig. 11. Variations of transmission bit rate versus effective refractive index at the assumed set of parameters.

vii) Figs. 7 has indicated that both modulator length and modulator capacitance increase, this results in decreasing of cut-off frequency.

viii) As shown in Fig. 8 has assured that as modulator width increases and modulator capacitance decreases, this leads to increase of cut-off frequency.

ix) Fig. 9 has indicated that both modulator length and modulator capacitance increase, this results in decreasing of 3-dB bandwidth.

x) As shown in Fig. 10 has demonstrated that as both modulator length and power absorption coefficient increase, this leads to decrease of modulation bandwidth.

xi) Fig. 11 has proved that as effective relative refractive-index change and modulator length increases, this effects in decreasing in transmission bit rates of modulator devices.

IV. CONCLUSIONS

The modulator device performance parameters have been described. It is evident that of both operating optical signal wavelength and power absorption coefficient this leads to the decreased switching voltage and then the increased modulator device performance index. It is also found theoretically that the decreased gap between electrodes and the increased confinement factor this results in the increased modulator device performance index. It is observed that the decreased of both modulator length and power absorption coefficient this leads to the increased of modulator device transmittance. Moreover the increased of both modulator thickness and width this results in the decreased of time constant of the modulator device operation. As well as the decreased of both modulator capacitance and modulator length and the increased modulator width this leads to the increased cut-off frequency of the modulator devices. In the same way, we have indicated that the decreased of modulator length, modulator capacitance, power absorption coefficient, and effective relative refractive change this results in the increased of the 3-dB bandwidth, modulation bandwidth and transmission bit rates of the modulator devices.

REFERENCES

[1] M. Sugiyama, M. Doi, S. Taniguchi, T. Nakazawa, and H. Onaka, "Driver-less 40 Gb/s LiNbO3 Modulator With Sub-1 V Drive Voltage," in Tech. Digest, Optical Fiber Communication Conference, PD FB6-2, 2002.

[2] N. Courjal, H. Porte, A. Martinez, and J.-P. Goedgebuer, "LiNbO3 Mach-Zehnder Modulator With Chirp Adjusted by Ferroelectric Domain Inversion," IEEE Photon. Tech. Lett., Vol. 14, No. 3, pp. 1509–1511, 2002.

[3] S. Shimotsu, S. Oikawa, T. Saitou, N. Mitsugi, , K. Kubodera, T. Kawanishi, and M. Izutsu, "Single Side Band Modulation Performance of a LiNbO3 Integrated Modulator Consisting of Four Phase Modulator Waveguides," IEEE Photon. Tech. Lett., Vol. 13, No. 5, pp. 364–366, 2001.

[4] S. Oikawa, T. Kawanishi, K. Higuma, Y. Matsuo, and M. Izutsu, "Double Stub Structure for Resonant Type Optical Modulators Using 20-m Thick Electrode," IEEE Photon. Tech. Lett., Vol. 15, No. 2, pp. 221–223, 2003.

[5] J. Kondo, K. Aoki, A. kondo, T. Eiiri, Y. Iwata, A. Hamajima, T. Mori, Y. Mizuno, M. Imaeda, Y. Kozuka, O. Mitomi, and M. Minakata, "High Speed and Low Driving Voltage Thin Sheet X-cut LiNbO3 Modulator With Laminated Low Dielectric Constant Adhesive," IEEE Photon. Tech. Lett., Vol. 17, No. 10, pp. 2077–2079, 2005.

[6] G. L. Li, S. A. Pappert, C. K. Sun, W. S. C. Chang, and P. K. L. Yu, "Wide Bandwidth Travelling Wave InGaAsP/InP Electro Absorption Modulator for Millimeter Wave Applications," in IEEE MTT-S Int. Microwave Symp. Dig., pp. 61–64, May 2001.

[7] H. Kawanishi, N. Mineo, Y. Shibuya, H. Murai, K. Yamada, and H.Wada, "EAM Integrated DFB Laser Modules With More Than 40 GHz Bandwidth," IEEE Photon. Technol. Lett., Vol. 13, No. 2, pp. 954–956, 2001.

[8] Ali W. Elshaari , and Stefan F. Preble, "10 Gbit/sec Broadband Silicon Electro-optic Absorption Modulator," Optics Communications, Vol. 28, No. 3, pp. 2829–2834, Mar. 2010.

[9] H. V. Pham, and Y. Okamura, "Electrooptic Modulators with Controlled Frequency Responses by Using Nonperiodically Polarization Reversed Structure," Journal of Advances in Optoelectronics, Vol. 8 , No. 1, pp. 1-8, 2008.

[10] T. Kawanishi, T. Sakamoto, and M. Izutsu, "High Speed Control of Lightwave Amplitude, Phase, and Frequency by use of Electrooptic Effect," IEEE Journal of Selected Topics in Quantum Electronics, Vol. 13, No. 1, pp. 79–91, 2007.

[11] H. V. Pham, H. Murata, and Y. Okamura, "Travelling Wave Electrooptic Modulators With Arbitrary Frequency Response Utilising Non Periodic Polarization Reversal," Electronics Letters, Vol. 43, No. 24, pp. 1379–1381, 2007.

[12] Ahmed Nabih Zaki Rashed, and Abd El-Fattah A. Saad, "Different Electro-Optical Modulators For High Transmission-Data Rates And Signal-Quality Enhancement," Journal of Russian Laser Research, Vol. 34, No. 4, pp. 336-345, July 2013.

[13] M. V. Raghavendra, P. H. Prasad, "Estimation of Optical Link Length for Multi Haul Applications," International Journal of Engineering Science and Technology, Vol. 2, No.6, pp. 1485-1491, 2010.

[14] Ahmed Nabih Zaki Rashed, "High reliability optical interconnections for short range applications in high performance optical communication systems," Optics and Laser Technology, Elsevier Publisher, Vol. 48, pp. 302–308, 2013.

[15] H. Hu, R. Ricken, W. Sohler, and R. Wehrspohn. "Lithium Niobate Ridge Waveguides Fabricated by Wet Etching,". IEEE Photonics Technology Letters, Vol. 19, No. 6, pp. 417-419, 2007.

[16] Ahmed Nabih Zaki Rashed, "Performance signature and optical signal processing of high speed electro-optic modulators," Optics Communications, Elsevier Publisher, Vol. 294, pp. 49-58, May 2013.

[17] R. L. Espinola, J. I. Dadap, R. M. Osgood Jr., S. J. McNab, and Y. A. Vlasov, "C-band wavelength conversion in silicon photonic wire waveguides," Optics Express, vol. 13, no. 11, pp. 4341–4349, 2005.

[18] K.Noguchi, O.Mitomi,H.Miyazawa and S.Seki,"A broadband Ti:LiNbO3 optical modulator with a ridge structure," J. Lighiwave Technol., Vol. 13, No. 3, pp.1 164-1168, 1995.

